

# NJC

Accepted Manuscript



This is an *Accepted Manuscript*, which has been through the Royal Society of Chemistry peer review process and has been accepted for publication.

*Accepted Manuscripts* are published online shortly after acceptance, before technical editing, formatting and proof reading. Using this free service, authors can make their results available to the community, in citable form, before we publish the edited article. We will replace this *Accepted Manuscript* with the edited and formatted *Advance Article* as soon as it is available.

You can find more information about *Accepted Manuscripts* in the [Information for Authors](#).

Please note that technical editing may introduce minor changes to the text and/or graphics, which may alter content. The journal's standard [Terms & Conditions](#) and the [Ethical guidelines](#) still apply. In no event shall the Royal Society of Chemistry be held responsible for any errors or omissions in this *Accepted Manuscript* or any consequences arising from the use of any information it contains.



[www.rsc.org/njc](http://www.rsc.org/njc)

1 **Study on the interaction characteristics of dexamethasone**  
2 **sodium phosphate with bovine serum albumin by spectroscopic**  
3 **technique**

4 Qian Wang, Xuyang Liu, Ming Su, Zhihong Shi and Hanwen Sun\*

5 College of Chemistry and Environmental Science, Hebei University; Key Laboratory of  
6 Analytical Science and Technology of Hebei Province, Baoding 071002, P. R. China.

7 The interaction of dexamethasone sodium phosphate (DEX-P) with bovine  
8 serum albumin (BSA) was studied by fluorescence quenching in  
9 combination with UV-Vis spectroscopic method under near physiological  
10 conditions. The fluorescence quenching rate constants and binding constants  
11 for BSA–DEX-P system were determined at different temperatures. The  
12 fluorescence quenching of BSA by DEX-P is due to static quenching and  
13 energy transfer. The results of thermodynamic parameters,  $\Delta H$  (-161.0 kJ  
14 /mol),  $\Delta S$  (-468.0 J/mol K) and  $\Delta G$  (-21.54~-16.86 kJ/mol), indicated that  
15 van der Waals interaction and hydrogen bonding played a major role for  
16 DEX-P–BSA association. The competitive experiments demonstrated that  
17 the primary binding site of DEX-P on BSA was located at site III in  
18 sub-domain III<sub>A</sub> of BSA. The distance between BSA and DEX-P is  
19 estimated to be 1.23 nm based on the Förster resonance energy transfer  
20 theory. The binding constant ( $K_a$ ) of BSA–DEX-P at 298 K was  $2.239 \times 10^4$

---

\* Corresponding author. Tel.: +86 312 5079719; Fax: +86 312 5079739.  
E-mail address: [hanwen@hbu.cn](mailto:hanwen@hbu.cn)

21 L/mol. Circular dichroism spectra, synchronous fluorescence and  
22 three-dimensional fluorescence studies showed that the presence of DEX-P  
23 could change the conformation of BSA during the binding process.

24 **KEYWORDS:** Fluorescence; Bovine serum albumin; Dexamethasone  
25 sodium phosphate; Interaction characteristics

## 26 **1. Introduction**

27 Serum albumin is one of the most abundant proteins in circulatory  
28 system of a wide variety of organisms and one of the most extensively  
29 studied proteins at all. The albumins make a significant contribution to  
30 colloid osmotic blood pressure and aid in the transport, distribution and  
31 metabolism of many endogenous and exogenous ligands. Protein–drug  
32 binding greatly influences absorption, distribution, metabolism and excretion  
33 properties of typical drugs[1]. Protein binding has long been considered one  
34 of the most important physicochemical characteristics of drugs, playing a  
35 potential role in distribution, excretion and therapeutic effectiveness.  
36 Dexamethasone (DEX) is a glucocorticoid and belongs to a group of  
37 medicines called corticosteroids. Dexamethasone sodium phosphate (DEX-P)  
38 is a water-soluble prodrug that is administered parenterally. Under  
39 physiological conditions, DEX-P exists principally as a di-anion. Its aqueous  
40 solubility and charge render DEX-P a much better candidate for transdermal  
41 iontophoretic delivery than the parent molecule (DEX)[2]. DEX-P is rapidly  
42 absorbed after oral administration and up to 65% of a dose is excreted in the

43 urine in 24 h. The plasma concentration of DEX-P was found to be highest  
44 (3  $\mu\text{g/L}$ ) at 4 h, declining rapidly to about 0.5  $\mu\text{g/L}$  at 24 h [3]. Thereby, it is  
45 important and necessary to study the interaction of DEX-P with serum  
46 albumins at molecular level.

47 Several methods have been applied to drug–protein binding studies  
48 among them equilibrium dialysis (ED) is considered as a reference method,  
49 However, ED suffers from many drawbacks such as low throughput,  
50 nonspecific adsorption to dialysis membrane, volume shifts, the Donnan  
51 effect, and it additionally requires sensitive analytical method for the  
52 determination of free drug concentration[4]. Capillary electrophoresis in the  
53 frontal analysis mode (CE/FA) is a promising technique for assessment of  
54 drug–protein interaction. This method offers certain advantages over the  
55 traditional ones such as simplicity, low sample requirements and  
56 consumption, short analysis times, high separation efficiencies, and high  
57 sample throughput[5]. Fluorescence spectroscopy is an effective tool for the  
58 investigation of conformational changes of protein under physiological  
59 conditions because of its accuracy, sensitivity, rapidity and convenience [6].  
60 It can reveal the accessibility of drugs to albumin's fluorophores, which can  
61 help us to understand the binding mechanisms of albumin–drug and to  
62 provide information on the structural features for determining the therapeutic  
63 effectiveness of the drug. However, one of the major problems associated  
64 with measurement of fluorescent organic matter in natural samples is the

65 inner-filter effect (IFE), sometimes referred to as self-absorption [7].  
66 The overall human plasma protein binding of DEX has been investigated by  
67 ED and the results suggested that the binding was linear and existed primary  
68 to albumin with little or no binding to corticosteroid binding globulin [8].  
69 The HSA-DEX interaction was also evaluated using the capillary  
70 electrophoresis/frontal analysis (CE/FA) [9]. A study was designed to  
71 examine the interaction of DEX-P with BSA and HSA under simulated  
72 physiological conditions in terms of buffer composition and protein  
73 concentration. The binding parameters obtained from the CE/FA experiment  
74 were compared to the ones calculated [10]. In another study, the interactions  
75 of DEX with low concentrations of BSA and HSA were examined by a  
76 fluorescence quenching and Fourier transformation infrared spectroscopy,  
77 and both the binding and thermodynamic parameters were calculated, but  
78 not correction of the inner-filter effect[11].

79 **Figure 1.** Chemical structure of dexamethasone sodium phosphate

80 In this work, DEX-P was selected as model drug (Figure 1), because it  
81 is a much better candidate for transdermal iontophoretic delivery than the  
82 parent molecule (DEX) [2]. To provide important insight into the interaction  
83 of the physiologically important protein BSA with drugs, this study  
84 examined, for the first time, the interaction between BSA and DEX-P under  
85 near physiological conditions by the fluorescence quenching in combination  
86 with UV-Vis spectroscopic method.

## 87 **2. Experimental**

### 88 **2.1. Drugs and reagents**

89 Commercially available bovine serum albumin (BSA, catalog no.  
90 A-7030, purity: 98%, M: 68000. BSA stock solution ( $1.0 \times 10^{-4}$  M) was  
91 prepared by dissolving an appropriate amount of BSA with 0.1 M Tris–HCl  
92 (pH 7.4) buffer solution, and kept in the dark at 4 °C. BSA working  
93 solutions were prepared by diluting the stock solution with water. DEX-P  
94 (purity: 98.7%) was purchased from the Jinyue Pharmacy Factory (Tianjin,  
95 China). A stock solution ( $1.0 \times 10^{-3}$  M) of DEX-P was prepared in water, and  
96 stored in refrigerator at –4 °C. Tris–HCl buffer (pH 7.40) consists of Tris  
97 (0.1 M) and HCl (0.1 M), and NaCl solution (0.5 M) was used to maintain  
98 the ion strength. All chemicals were of analytical reagent grade or better.  
99 Purified water was prepared by an XGJ-30 highly pure water machine  
100 (Yongcheng purification Science & Technology Co. Ltd., Beijing, China).

### 101 **2.2. Equipment**

102 All fluorescence measurements were performed on an F-7000  
103 Fluorescence spectrophotometer (Hitachi, Japan) which was equipped with a  
104 1 cm quartz cell and thermostat bath. The spectrum data points were  
105 collected from 280 to 500 nm. The widths of the excitation and the emission  
106 slit were both set at 5 nm. Fluorescence measurements were carried out at  
107 room temperatures.

108 Circular dichroism (CD) spectra were obtained on a MOS-450/SFM300  
109 circular dichroism spectrometer (Bio-Logic Com. Germany). The absorption  
110 spectra were performed on an TU-1900 double light Spectrophotometer  
111 (Beijing TAYASAF Science & Technology Co., Ltd, China) using a 1 cm  
112 quartz cell in the wavelength range of 200–500 nm. All pH measurements  
113 were performed with a PHS-3C pH meter (Shanghai, China).

### 114 **2.3. Determination of fluorescence intensity**

115 Five 10-mL clean and dried test tubes were taken, and 2 mL of 0.5 M  
116 NaCl, 2.0 mL Tris–HCl buffer (pH 7.40), 0.25 mL of  $4.0 \times 10^{-5}$  M BSA, and  
117 different volumes (2.0–4.0 mL) of DEX-P standard solution of  $1.936 \times 10^{-4}$   
118 M were added in each test tube, and diluted to 10 mL with water. The  
119 concentration of BSA was  $1.0 \times 10^{-6}$  M, and that of DEX-P was 9.5, 19, 28.5,  
120 38.0, and  $47.5 \times 10^{-6}$  M. Sixth test-tube containing only BSA solution at pH  
121 7.4 was marked as “control”, and seventh test-tube containing only  
122  $9.5 \times 10^{-6}$  M DEX-P was used for the comparison. After mixing the solutions,  
123 these were allowed to stand for 15 min for maximum binding of DEX-P to  
124 BSA. The fluorescence intensity after the correction of inner-filter effect was  
125 calculated by the equation [12]:  $F_{cor} = F_{obs} \exp(\frac{1}{2}A_{ex} + \frac{1}{2}A_{em})$ , where  $F_{obs}$  is  
126 fluorescence intensity measured before the correction of inner-filter effect,  
127  $A_{ex}$  and  $A_{em}$  are absorbance of the test solution at excitation and emission  
128 wavelengths, respectively. The corrected fluorescence intensity was used for  
129 studying on the interaction of DEX-P and BSA. After corrected inner-filter

130 effect, fluorescence intensity ( $F_0$ ) in the absence of quencher DEX-P and the  
131 fluorescence intensity ( $F$ ) in the presence of quencher DEX-P were  
132 measured at a wavelength of  $\lambda_{ex}$  280 nm and  $\lambda_{em}$  340 nm under  
133 temperature of 298, 303 and 308 K for estimating the interaction between  
134 DEX-P and BSA.

### 135 3. Results and discussion

#### 136 3.1. Fluorescence quenching mechanism

137 Fluorescence quenching refers to any process that decreases the  
138 fluorescence intensity of a sample. A variety of molecular interactions can  
139 result in fluorescence quenching of excited state fluorophores. These include  
140 molecular rearrangements, energy transfer, ground state complex formation  
141 and collisional quenching. Figure 2 shows the fluorescence spectra of BSA  
142 in the absence and presence of DEX-P after corrected inner-filter effect.

143 **Figure 2.** Fluorescence spectra of BSA in the absence or presence of DEX-P at  $\lambda_{ex}$   
144 280 nm and 298K after corrected inner-filter effect and absorption spectra  
145 a→f: BSA,  $1.0 \times 10^{-6}$  M; DEX-P ( $\times 10^{-6}$  M), 0, 9.5, 19, 28.5, 38.0 and 47.5; For  
146 inner-filter effect, their absorbance at  $\lambda_{ex}$  280 nm were 0.018, 0.048., 0.070,  
147 0.103, 0.130 and 0.159, and absorbance at  $\lambda_{em}$  340 nm were 0.008, 0.009,  
148 0.008, 0.011, 0.011 and 0.012, respectively; g: DEX-P,  $9.5 \times 10^{-6}$  M; 0.1 M NaCl,  
149 0.02 M Tris-HCl buffer (pH 7.40)

150 No fluorescence of DEX-P was observed. The fluorescence spectra of  
151 BSA show a broad band with maximum at  $\sim 340$  nm. It is observed that both  
152 fluorescence intensity decreases and absorbance of BSA increases with  
153 increasing concentration of DEX-P. A maximum fluorescence emission of  
154 BSA underwent spectral shift from 340 to 345 nm, and a maximum

155 absorption of BSA underwent spectral shift slightly. It is suggested that BSA  
156 and DEX-P formed a complex, and an energy transfer between DEX-P and  
157 BSA occurred.

158 The fluorescence quenching data are analyzed by the Stern–Volmer  
159 equation [13]:

$$160 \quad F_0/F = 1+k_q\tau_0[Q] = 1+k_{sv}[Q] \quad (1)$$

161 where  $F_0$  and  $F$  are the fluorescence intensity in the absence and presence of  
162 quencher, respectively.  $k_q$  is the quenching rate constant,  $\tau_0$  is the  
163 fluorescence life time of biopolymer BSA ( $\tau_0=10^{-8}$  s)[14],  $k_{sv}$  and  $[Q]$  are the  
164 Stern–Volmer quenching constant and concentration of quencher,  
165 respectively.

166 In this work, the Stern–Volmer plots of  $F_0/F$  vs concentration of  
167 DEX-P were obtained (Fig.3). The values estimated are given in Table 1.

168 **Figure 3.** Stern-Volmer plots of  $F_0/F$  vs concentration of DEX-P under different  
169 temperatures after corrected inner-filter effect  
170  $F_0/F$  data are average with relative standard deviation of 6.9, 8.5 and 8.9% at  
171 298, 303 and 308 K, respectively.

172 **Table 1.** Quenching parameter of BSA–DEX-P at different temperatures

173 The variation of  $F_0/F$  against DEX-P concentration  $Q$  fits in the  
174 equation of  $y = m x + c$  with correlation coefficient (R) greater than 0.99.  
175 Obviously, the quenching parameters are the lack of temperature  
176 dependence, and the rate constants  $k_q$  at temperature ranged from 298 to 308  
177 K greater than the maximum scatter collision quenching constants of various  
178 quenchers with the biomolecule ( $2.0 \times 10^{10}$  L/mol s)[15], which suggests that

179 the quenching is not initiated by dynamic quenching but by static quenching  
180 resulted from the formation of a complex.

### 181 **3.2. Binding constant and binding site number**

182 The binding of DEX-P with BSA to form complex in the ground state is  
183 further understood on the basis of available binding site number and binding  
184 constant of the complex formation process. For static quenching, the  
185 following equation was used to calculate the binding constant and binding  
186 sites [16,17]:

$$187 \quad \log[(F_0 - F)/F] = \log K_a + n \log [Q] \quad (2)$$

188 where  $K_a$  and  $n$  are the binding constant and binding site number,  
189 respectively. The plots of  $\log [(F_0 - F)/F]$  vs  $\log [Q]$  are linear. Binding  
190 constant ( $K_a$ ) and the binding site number ( $n$ ) could be calculated from the  
191 intercept and slope, as shown in Table 2.

192 **Table 2.** Regression equation, correlation coefficient (R), binding constant  $K_a$  and the  
193 number of binding site  $n$  between DEX-P and BSA at different temperatures

194 It was noticed that the binding constant values decreased with increase in  
195 temperature due to reduction of the stability of DEX-P–BSA complexes. The  
196 binding constants of DEX-P and BSA in the temperature range of 298–308  
197 K ranged from  $2.239 \times 10^4$  to  $6.918 \times 10^2$  L/mol. The average value of DEX-P  
198 and BSA was  $8.18 \times 10^3$  L/mol. It is of the same order of magnitude as the  
199 binding constant ( $7.87 \times 10^3$  L/mol) obtained for DEX-P–BSA using CE/FA  
200 and that ( $2.22 \times 10^3$  L/mol) reported using ED for DEX-P–BSA [10].  
201 Otherwise, the binding constants of DEX-P–BSA and DEX–HAS/BSA are

202 near[9,11], showing DEX-P and DEX having similar bioactivity.

### 203 3.3. Interaction forces between DEX-P with BSA

204 The interaction forces between drug and biomolecules include  
205 hydrogen bonds, van der Waals forces, electrostatic and hydrophobic  
206 interactions[18]. The temperature dependence of the interaction of DEX-P  
207 with BSA was investigated at 298, 303 and 308 K. The thermodynamic  
208 parameters can be evaluated from the Van't Hoff equation:

$$209 \quad \ln K_a = -\Delta H/RT + \Delta S/R \quad (3)$$

210 where  $K_a$  is the binding constant at corresponding temperature T, and R is  
211 the gas constant. The enthalpy change ( $\Delta H$ ) and entropy change ( $\Delta S$ ) can be  
212 obtained from the slope and the ordinates at the origin of the Van't Hoff plot,  
213 respectively (Fig.4).

214 The free energy change,  $\Delta G$  is determined from the following  
215 relationship

$$216 \quad \Delta G = \Delta H - T\Delta S \quad (4)$$

217 The values of  $\Delta G$ ,  $\Delta S$  and  $\Delta H$  are calculated and summarized in Table 3.

218 **Figure 4.** Van't Hoff plot for the interaction of DEX-P with BSA in 0.02 M  
219 Tris-HCl buffer (pH 7.40)-0.1 M NaCl solution at 298, 303 and 308 K and pH  
220 7.40.

221 **Table 3.** Thermodynamic parameters of the interaction between DEX-P and BSA at  
222 different temperatures

223 The negative values of free energy ( $\Delta G$ ) supports the assertion that the  
224 binding process is spontaneous. The negative enthalpy ( $\Delta H$ ) and entropy ( $\Delta S$ )  
225 values of the interaction of DEX-P and BSA indicate that the binding is

226 mainly enthalpy-driven and the entropy is unfavorable for it. This is similar  
227 with the interaction of DEX and BSA [11]. So Van der Waals interaction  
228 and hydrogen bond play major roles in the binding process [19].

### 229 **3.4. Binding site of DEX-P on BSA**

230 BSA has two tryptophan residues, Trp-212 and Trp-134. Similar to HSA,  
231 Trp-212 is located in subdomain IIA whereas Trp-134 is localized in the  
232 sub-domain IA [20]. On the basis of the probe-displacement method, there  
233 are at least three relatively-high specific drug-binding sites on the BSA  
234 molecules. These sites, commonly called warfarin, ibuprofen and  
235 digoxin-binding sites, are also denoted as Site I, Site II, and Site III,  
236 respectively[21,22]. To further determine the binding site of DEX-P, the  
237 competitive experiments were carried out at a temperature of 298 K using  
238 warfarin, ibuprofen and digoxin as a Site I-, Site II- and Site III-specific  
239 probe, respectively. The concentration ratio of BSA and probe was 1:1  
240 ( $2 \times 10^{-6}$  M:  $2 \times 10^{-6}$  M). The plots of  $\log [(F_0 - F)/F]$  vs  $\log [C_{DEX-P}]$  in the  
241 absence and presence of site specific probe were prepared. The values of  
242 binding constant ( $K_a$ ) and the binding site number ( $n$ ) were calculated from  
243 the intercept and slope based on the Eq. (2). Binding constant and the  
244 binding site number were obtained.

245 **Table 4.** Binding constant  $K_a$  and binding site number  $n$  between DEX-P and BSA  
246 in the presence of site-specific probe

247 The data in Table 4 show that the binding constants for DEX-P–BSA  
248 system were  $2.239 \times 10^4$  L/mol, while in the presence of site specific probe  
249 the binding constants decreased obviously. In the digoxin probe case, the  
250 binding constants decreased to  $3.412 \times 10^3$  L/mol. It is shown the competition  
251 of digoxin with DEX-P at a same site. The competitive experiments  
252 suggested that the primary binding site of DEX-P on BSA was located at site  
253 III in sub-domain III<sub>A</sub> of BSA.

### 254 3.5. Energy transfer from BSA to DEX-P

255 Fluorescence resonance energy transfer is an important technique for  
256 investigating a variety of biological phenomena including energy transfer  
257 processes[23]. Here the donor and acceptor are BSA and DEX-P,  
258 respectively. It was observed that there is spectral overlap between  
259 fluorescence emission of BSA and absorption spectra of DEX-P in the  
260 wavelength range of 285–450 nm, as shown in Fig. 5.

261 **Figure 5.** Spectral overlap of DEX-P absorption with BSA fluorescence in 0.02 M  
262 Tris–HCl buffer (pH 7.40) –0.1 M NaCl solution at 298 K  
263 (a) absorption spectra of DEX-P; (b) fluorescence spectra of BSA-DEX-P; (c)  
264 fluorescence spectra of BSA; DEX-P,  $1.0 \times 10^{-6}$  M; BSA,  $1.0 \times 10^{-6}$  M

265 The fluorescence emission of BSA–DEX-P solution at an excitation  
266 wavelength of 280 nm is from BSA only since DEX-P is a non-fluorescence  
267 drug molecule. However, at this wavelength DEX-P has weak absorption. It  
268 suggested the possibility of fluorescence resonance energy transfer from  
269 BSA to DEX-P molecules in solution.

270 The region of integral overlap is used to calculate the critical energy  
271 transfer distance ( $R_0$ ) between BSA (donor) and DEX-P (acceptor) according  
272 to Foster's non-radioactive energy transfer theory using Förster's  
273 equation[16,24]. Based on this theory, the efficiency ( $E$ ) of energy transfer  
274 between donor (BSA) and acceptor (DEX-P) can be calculated by Equation  
275 (3):

$$276 \quad E = R_0^6 / (R_0^6 + r^6) \quad (3)$$

277 Where,  $r$  is the binding distance between donor and acceptor, and  $R_0$  is the  
278 critical binding distance. When the efficiency ( $E$ ) of energy transfer is 50%,  
279 which can be calculated by Equation (4):

$$280 \quad R_0^6 = 8.8 \times 10^{-25} k^2 n^{-4} \Phi_D J \quad (4)$$

281 Where, the  $k^2$  is the spatial orientation factor of the dipole,  $n$  is the refractive  
282 index of medium,  $\Phi_D$  is the quantum yield of the donor in the absence of  
283 acceptor and  $J$  is the overlap integral of the emission spectrum of the donor  
284 and the absorption spectrum of the acceptor. The  $J$  can be calculated by  
285 Equation:

$$286 \quad J = \sum F(\lambda) \varepsilon(\lambda) \lambda^4 \Delta\lambda / \sum F(\lambda) \Delta\lambda \quad (5)$$

287 Where,  $F(\lambda)$  is the fluorescence intensity of the fluorescent donor of  
288 wavelength,  $\lambda$ ,  $\varepsilon(\lambda)$  is the molar absorption coefficient of the acceptor at  
289 wavelength,  $\lambda$ . In the present case,  $k^2$ ,  $n$  and  $\Phi_D$  are 2/3, 1.336 and 0.118,  
290 respectively [25].

291 The efficiency ( $E$ ) of energy transfer can be determined by Equation:

292 
$$E = 1 - F/F_0 \quad (6)$$

293 Where,  $F_0$  and  $F$  are the fluorescence intensities of BSA solutions in the  
294 absence and presence of DEX-P, respectively.

295 From the overlapping we found  $R_0 = 0.79$  nm from Eq. (4) using  $k^2 =$   
296  $2/3$ ,  $n = 1.336$  and  $\Phi_D = 0.118$  (tryptophan residue) for the aqueous solution  
297 of BSA.  $J$  could be calculated from Eq. (5) and the corresponding result was  
298  $7.278 \times 10^{-18}$  cm<sup>3</sup>/mol.  $E$  calculated from Eq. (6) was 4.452%. At the same  
299 time, the binding distance ( $r$ ) between BSA and DEX-P was obtained to be  
300 1.23 nm by Eq. (3). The donor-to-acceptor distance,  $r < 8$  nm, indicated that  
301 the energy transfer from BSA to DEX-P occurs with high possibility[26]. It  
302 also suggested that the bindings of DEX-P to BSA molecules were formed  
303 through energy transfer, which quenched the fluorescence of BSA molecules,  
304 indicating the presence of static quenching interaction between BSA and  
305 DEX-P.

### 306 **3.6. Change of BSA conformation**

#### 307 **3.6.1. Circular dichroism studies**

308 Circular dichroism is a sensitive technique to monitor conformational  
309 changes in protein structure[28]. CD spectra of BSA and BSA-DEX-P are  
310 shown in Fig.6.

311 **Figure 6.** CD spectra of BSA and BSA-DEX-P in 0.02 M Tris-HCl buffer (pH  
312 7.40)-0.1 M NaCl solution at 298 K  
313 (a) BSA,  $1.0 \times 10^{-6}$ M; (b) BSA/DEX-P,  $1.0 \times 10^{-6}$ M/ $1.0 \times 10^{-6}$ M

314 In BSA spectrum, there are negative peaks in the ultraviolet region, one  
315 at 209 nm and the other at 222 nm, which are characteristic of the  $\alpha$ -helical  
316 structure of a protein. Trynda-Lemiesz et al. explained that both of the  
317 negative peaks between 208-209 and 222-223 nm contribute to the transfer  
318 for the peptide bond of the  $\alpha$ -helix[27]. In the presence of DEX-P, the  
319 intensity of both the negative peaks increased slightly, proving the change of  
320 the  $\alpha$ -helical structure of BSA due to the formed complex of BSA and  
321 DEX-P. The CD spectra observed for BSA in the presence of DEX-P are  
322 similar in shape, indicating that the structure of BSA is also predominantly  
323  $\alpha$ -helical[28].

### 324 3.6.2. Synchronous fluorescence spectral change of BSA

325 Synchronous fluorescence is a kind of simple and sensitive method to  
326 measure the fluorescence quenching. It can provide the information of  
327 polarity change around the chromophore micro-environment.  $\Delta\lambda$ ,  
328 representing the difference between excitation and emission wavelengths, is  
329 an important operating parameter. When  $\Delta\lambda$  is 15 nm, synchronous  
330 fluorescence is characteristic of tyrosine residue, while when  $\Delta\lambda$  is 60 nm, it  
331 provided the characteristic information of tryptophan residues[29]. The  
332 synchronous fluorescence spectra of tyrosine residue and tryptophan  
333 residues in BSA with addition of DEX-P were observed, as shown in Fig. 7.

334 **Figure 7.** Synchronous fluorescence spectra of BSA with different amount of  
335 DEX-P in 0.02 M Tris-HCl buffer (pH 7.40)-0.1 M NaCl solution at 298  
336 K

337 (A)  $\Delta\lambda=15$  nm, and (B)  $\Delta\lambda=60$  nm; T=298K; a→f: BSA,  $1.0\times 10^{-6}$ M;  
338 DEX-P( $10^{-6}$  M), 0, 9.5, 19, 28.5, 38.0, and 47.5

339 When the drug DEX-P was gradually added, the peak wavelength of  
340 tyrosine residues ( $\Delta\lambda=15$  nm) did not change, and the fluorescence intensity  
341 decreased regularly. Otherwise, the peak of tryptophan residues ( $\Delta\lambda=60$  nm)  
342 in BSA underwent spectral shift, and the fluorescence intensity and the pitch  
343 of quenching for  $\Delta\lambda=60$  nm was much higher than those for  $\Delta\lambda=15$  nm.  
344 Such result means DEX-P is closer to tryptophan residues than tyrosine  
345 residues, namely binding sites mainly are focused on tryptophan moiety.

### 346 3.6.3. Three-dimensional fluorescence spectral change of BSA

347 The three-dimensional fluorescence spectrum is another powerful  
348 method for studying conformation change of BSA. In this work, the  
349 three-dimensional fluorescence spectra and the contour spectra of BSA and  
350 BSA–DEX-P systems were observed, as shown in Fig. 8, and the  
351 characteristic parameters are summarized in Table 5.

352 **Figure 8.** Three-dimensional fluorescence spectra of (A) and contour spectra (B) of  
353 BSA and BSA–DEX-P systems in 0.02 M Tris–HCl buffer (pH 7.40)–0.1 M  
354 NaCl solution at 298 K  
355 A-1 and B-1: BSA,  $1\times 10^{-6}$ M; A-2 and B-2: BSA–DEX-P,  $1\times 10^{-6}$ M/ $4\times 10^{-5}$ M,

356 **Table 5.** Three-dimensional fluorescence spectra characteristic parameters of the BSA  
357 and BSA–DEX-P systems

358 From Fig. 8, peak 1 ( $\lambda_{ex}/\lambda_{em}=225/340$  nm) reveals the spectral  
359 characteristic of tryptophan and tyrosine residues. After the addition of  
360 DEX-P, the fluorescence intensity of BSA decreased from 174.2 to 42.69.  
361 This suggests a less polar environment of both residues and almost all the

362 hydrophobic amino acid residues of BSA were buried in the hydrophobic  
363 pocket. Less polar environment means that the binding position between  
364 DEX-P and BSA located within this hydrophobic pocket, the addition of  
365 DEX-P changed the polarity of this hydrophobic microenvironment and the  
366 conformation of BSA[30]. In Fig. 8, peak 2 ( $\lambda_{ex}/\lambda_{em} = 275/340$  nm) reveals  
367 the fluorescence spectra behavior of polypeptide backbone structures, which  
368 is caused by the transition of  $\pi-\pi^*$  of BSA's characteristic polypeptide  
369 backbone structure C=O [31].

370 After the addition of DEX-P, the fluorescence intensity of BSA  
371 decreased from 170.9 to 87.36, and from the contour spectra in Fig.8, after  
372 addition of DEX-P in BSA, fingerprint lines of contour spectra changed to  
373 be sparse markedly. These revealed that the microenvironment and  
374 conformation of BSA were changed in the binding reaction. The interaction  
375 between DEX-P and BSA induced the unfolding of the polypeptides chains  
376 of BSA and conformational change of BSA.

#### 377 **4. Conclusions**

378 The results showed that dexamethasone sodium phosphate can bind to  
379 bovine serum albumin by hydrogen bonding and Van der Waals forces. The  
380 primary binding for dexamethasone sodium phosphate was located at site III  
381 in subdomain IIIA of bovine serum albumin. The result demonstrated that  
382 the presence of dexamethasone sodium phosphate induced some micro  
383 environmental and conformational changes of bovine serum albumin

384 molecules. Circular dichroism spectra, synchronous fluorescence and  
385 three-dimensional fluorescence studies showed that the presence of  
386 dexamethasone sodium phosphate could change the conformation of bovine  
387 serum albumin during the binding process. The results are of great  
388 importance in pharmacy, pharmacology and biochemistry, and are expected  
389 to provide important insight into the interactions of the physiologically  
390 important protein bovine serum albumin with drugs.

### 391 **Acknowledgements**

392 This work was supported by the Natural Science Found of Hebei Province  
393 (B2008000583) and the sustentation Plan of Science and Technology of  
394 Hebei Province (No. 10967126D).

### 395 **References**

- 396 [1] P.B. Kandagal, S.M.T. Shaikh, D.H. Manjunatha, J. Seetharamappa and  
397 B.S. Nagaralli, *J. Photochem. Photobiol. A*, 2007, **189**, 121–127.
- 398 [2] Y.N. Kalia, A. Naik, J. Garrison and R.H. Guy, *Adv. Drug. Deliv. Rev.*,  
399 2004, **56**, 619–658.
- 400 [3] A.C. Moffat (Ed.), *Clarke's Isolation and Identification of Drugs*, The  
401 Pharmaceutical Press, London, 1986.
- 402 [4] K. Vuignier, J. Schappler, J. L.Veuthey, P. A. Carrupt and S. Martel,  
403 *Anal. Bioanal. Chem.*, 2010, **398**, 53–66.

- 404 [5] P. He and H.W. Sun, *J. Hebei Univ. (Natural Science Edition)*, 2009, **29**,  
405 214-224.
- 406 [6] N. Li and Y.J. Wei, *J. Hebei Nor. Univ. (Natural Science Edition)*, 2003,  
407 **27**, 176–180.
- 408 [7] T. Larsson, M. Wedborg and D. Turner, *Anal. Chim. Acta*, 2007, **583**,  
409 357–363.
- 410 [8] D. M. Cummnngs, G. E.Larijani, D. P. Conner, R. K. Ferguson and M. L.  
411 Rocci Jr, *Ann. Pharmacother.*, 1990, **24**, 229–231.
- 412 [9] P.Zhao, G. Zhu, W. Zhang, L. Zhang, Z. Liang and Y. Zhang, *Anal.*  
413 *Bioanal. Chem.*, 2009, **393**, 257–261.
- 414 [10] A. Gonciarz , K. Kus, M. Szafarz, M. Walczak, A. Zakrzewska and J.  
415 Szymura-Oleksiak, *Electrophoresis*, 2012, **33**, 3323-3330.
- 416 [11] P. N. Naik, S. A. Chimatadar and S. T. Nandibewoor, *J. Photochem.*  
417 *photobiol. B: Biology*, 2010, **100**, 147–159.
- 418 [12] J. R. Lakowicz, Principles of fluorescence spectroscopy, 3rd edn.  
419 Springer Science+Business Media, New York. (2006)
- 420 [13] L.N. Zhang, F. Y. Wu and A.H. Liu, *Spectrochim. Acta A*, 2011, **79**,  
421 97–103.
- 422 [14] J.R. Lackowicz and G. Weber, *Biochem.*, 1973,**12**, 4161–4170.
- 423 [15] R.E. Maurice and A.G. Camillo, *Anal. Biochem.*, 1981, **114**, 199–212.
- 424 [16] Y.J. Hu, Y. Liu, R. M. Zhao, J.X. Dong and S. S. Qu, *J. Photochem.*  
425 *Photobiol. A*, 2006, **179**, 324–329.

- 426 [17] N.Barbero, E. Barni, C. Barolo, P. Quagliotto, G. Viscardi, L. Napione,  
427 S. Pavan and F. Bussolino, *Dyes Pigments*, 2009, **80**, 307–313.
- 428 [18] Y.Z. Zhang, X.X. Chen, J. Dai, X.P. Zhang, Y.X. Liu and Y. Liu, *Lumin.*,  
429 2008, **23**, 150 – 156.
- 430 [19] D.P. Ross and S. Subramanian, *Biochem.*, 1981, **20**, 3096 – 3102.
- 431 [20] J. Jayabharathi, V. Thanikachalam, R. Sathishkumar and K.  
432 Jayamoorthy, *J. Photochem. Photobiol. B: Biology*, 2012, **117**,  
433 222–227.
- 434 [21] U. Kragh-Hansen, *Pharmacol. Rev.*, 1981, 33, 17 – 53.
- 435 [22] N. Dubois, F. Lopicque, J. Magdalou, M. Abiteboul and P. Netter,  
436 *Biochem. Pharmacolo.*,1994, **48**, 1693–1699.
- 437 [23] A. Mallick, B. Haldar and N. Chattopadhyay, *J. Phys. Chem. B*, 2005,  
438 **109**, 14683–14690.
- 439 [24] S.L. Bhattar, G.B. Kolekar and S.R. Patil, *J. Lumin.*, 2008, **128**,  
440 306–310.
- 441 [25] S.M.T. Shaikh, J. Seetharamappa, P.B. Kandagal and S. Ashoka, *J. Mol.*  
442 *Struct.*, 2006, **786**, 46–52.
- 443 [26] X. C. Zhao, R.T. Liu, Z.X. Chi, Y. Teng and P.F. Qin, *J. Phys. Chem. B*,  
444 2010, **114**, 5625–5631.
- 445 [27] L. Trynda-Lemiesz, A. Karaczyn, B.K. Keppler and H.J. Kozlowski,  
446 *Inorg. Biochem.*, 2000, **78**, 341 – 346.

- 447 [28] Y.J. Hu, Y. Liu, X.S. Shen, X.Y. Fang and S.S. Qu, *J. Mol. Struct.*, 2005,  
448 **738**, 143 - 147.
- 449 [29] M. Guo, W.J. Lue, M.H. Li and W. Wang, *Eur. J. Med. Chem.*, 2008, **43**,  
450 2140–2148.
- 451 [30] X.J. Guo, X.D. Sun and S.K. Xu, *J. Mol. Struct.*, 2009, **931**, 55 - 59.
- 452 [31] Q. Xiao, S. Huang, Y. Liu, F.F. Tian and J.C. Zhu, *J. Fluoresc.*, 2009, **19**,  
453 317–326.
- 454
- 455
- 456
- 457
- 458
- 459
- 460
- 461
- 462
- 463
- 464
- 465
- 466
- 467
- 468

469

470 **List of figures**

471 Figure 1. Chemical structure of dexamethasone sodium phosphate

472 Figure 2. Fluorescence spectra of BSA in the absence or presence of DEX-P at  $\lambda_{ex}$  280  
473 nm and 298K after corrected inner-filter effect and absorption spectra474 a→f: BSA,  $1.0 \times 10^{-6}$  M; DEX-P ( $\times 10^{-6}$  M), 0, 9.5, 19, 28.5, 38.0 and 47.5; For  
475 inner-filter effect, their absorbance at  $\lambda_{ex}$  280 nm were 0.018, 0.048, 0.070, 0.103,  
476 0.130 and 0.159, and absorbance at  $\lambda_{em}$  340 nm were 0.008, 0.009, 0.008, 0.011,  
477 0.011 and 0.012, respectively; g: DEX-P,  $9.5 \times 10^{-6}$  M; 0.1 M NaCl, 0.02 M  
478 Tris-HCl buffer (pH 7.40)479 Figure 3. Stern-Volmer plots of  $F_0/F$  vs concentration of DEX-P under different  
480 temperatures after corrected inner-filter effect481  $F_0/F$  data are average with relative standard deviation of 6.9, 8.5 and 8.9% at 298,  
482 303 and 308 K, respectively.483 Figure 4. Van't Hoff plot for the interaction of DEX-P with BSA in 0.02 M Tris-HCl  
484 buffer (pH 7.40)–0.1 M NaCl solution at 298, 303 and 308 K and pH 7.40.485 Figure 5. Spectral overlap of DEX-P absorption with BSA fluorescence in 0.02 M  
486 Tris-HCl buffer (pH 7.40)–0.1 M NaCl solution at 298 K487 (a) absorption spectra of DEX-P; (b) fluorescence spectra of BSA-DEX-P; (c)  
488 fluorescence spectra of BSA; DEX-P,  $1.0 \times 10^{-6}$  M; BSA,  $1.0 \times 10^{-6}$  M489 Figure 6. CD spectra of BSA and BSA-DEX-P in 0.02 M Tris-HCl buffer (pH 7.40)–0.1  
490 M NaCl solution at 298 K491 (a) BSA,  $1.0 \times 10^{-6}$  M; (b) BSA/DEX-P,  $1.0 \times 10^{-6}$  M/ $1.0 \times 10^{-6}$  M492 Figure 7. Synchronous fluorescence spectra of BSA with different amount of DEX-P in  
493 0.02 M Tris-HCl buffer (pH 7.40)–0.1 M NaCl solution at 298 K494 (A)  $\Delta\lambda = 15$  nm, and (B)  $\Delta\lambda = 60$  nm; T=298K; a→f: BSA,  $1.0 \times 10^{-6}$  M;  
495 DEX-P ( $10^{-6}$  M), 0, 9.5, 19, 28.5, 38.0, and 47.5496 Figure 8. Three-dimensional fluorescence spectra of (A) and contour spectra (B) of BSA  
497 and BSA-DEX-P systems in 0.02 M Tris-HCl buffer (pH 7.40)–0.1 M NaCl  
498 solution at 298 K499 A-1 and B-1: BSA,  $1 \times 10^{-6}$  M; A-2 and B-2: BSA-DEX-P,  $1 \times 10^{-6}$  M/ $4 \times 10^{-5}$  M,  
500  
501  
502  
503  
504  
505  
506

507

508

509

510 **Table 1**

511 Quenching parameter of BSA–DEX-P at different temperatures

T (K)	Regression equation	R	$k_{sv}$ (L/mol)	$k_q$ (L/mol s)
298	$F_0/F=0.991+0.768\times 10^4 [Q]$	0.9971	$7.68\times 10^3$	$7.68\times 10^{11}$
303	$F_0/F=1.011+0.725\times 10^4 [Q]$	0.9900	$7.25\times 10^3$	$7.25\times 10^{11}$
308	$F_0/F=1.031+0.705\times 10^4 C [Q]$	0.9935	$7.05\times 10^3$	$7.05\times 10^{11}$

512

513

514

515

516

517

518

519

520

521

522

523

524

525

526

527

528

529

530

531

532

533

534

535

536

537

538

539

540

541

542

543

544

545

546

547  
548  
549  
550  
551  
552  
553  
554  
555  
556  
557  
558  
559  
560  
561  
562  
563  
564  
565  
566  
567  
568  
569  
570  
571  
572  
573  
574  
575  
576  
577  
578  
579  
580  
581  
582  
583  
584

**Table 2**

Regression equation, correlation coefficient (R), binding constant  $K_a$  and the number of binding site n between DEX-P and BSA at different temperatures

T (K)	Regression equation	R	$K_a$ (L/mol)*	n
298	$\log[(F_0-F)/F]=4.350+1.114 \log [Q]$	0.9963	$(2.239\pm 0.155)\times 10^4$	1.11
303	$\log[(F_0-F)/F]=3.160+0.8468 \log [Q]$	0.9918	$(1.445\pm 0.123)\times 10^3$	0.85
308	$\log[(F_0-F)/F]=2.840+0.7669 \log [Q]$	0.9915	$(6.918\pm 0.615)\times 10^2$	0.77

\* (average  $\pm$ Standard Deviation), n=3

585  
586  
587  
588  
589  
590  
591

**Table 3**

Thermodynamic parameters of the interaction between DEX-P and BSA at different temperatures

T (K)	$K_a$ (L/mol)	R	$\Delta H$ (kJ/mol)	$\Delta S$ (J/mol K)	$\Delta G$ (kJ/mol)
298	$2.239 \times 10^4$	0.9963	-161.0	-468.0	-21.54
303	$1.445 \times 10^3$	0.9918			-19.20
308	$6.918 \times 10^2$	0.9915			-16.86

592  
593  
594  
595  
596  
597  
598  
599  
600  
601  
602  
603  
604  
605  
606  
607  
608  
609  
610  
611  
612  
613  
614  
615  
616  
617  
618  
619  
620  
621  
622

623  
624  
625  
626  
627  
628  
629  
630  
631  
632  
633  
634  
635  
636  
637  
638  
639  
640  
641  
642  
643  
644  
645  
646  
647  
648  
649  
650  
651  
652  
653  
654  
655  
656

**Table 4**

Binding constant  $K_a$  and binding site number  $n$  between DEX-P and BSA in the presence of site-specific probe

System	$K_a$ (L/mol)	$n$	R
DEX-P-BSA	$2.239 \times 10^4$	1.11	0.9963
DEX-P-BSA-warfarin	$1.227 \times 10^4$	1.05	0.9962
DEX-P-BSA-ibuprofen	$8.710 \times 10^3$	1.03	0.9935
DEX-P-BSA-digoxin	$3.412 \times 10^3$	0.92	0.9939

657

658

659

660

661 **Table 5**662 Three-dimensional fluorescence spectra characteristic parameters of the BSA and  
663 BSA–DEX-P systems

Systems	Parameters	Peak 1	Peak 2
BSA	Peak position( $\lambda_{ex}/\lambda_{em}$ , nm)	225/340	275/340
	Relative intensity	174.2	170.9
	Stokes shift $\Delta\lambda$ (nm)	115	65
BSA–DEX-P	Peak position( $\lambda_{ex}/\lambda_{em}$ , nm)	225/335	285/340
	Relative intensity	42.69	87.36
	Stokes shift $\Delta\lambda$ (nm)	110	55

664

665

666

667

668

669

670

671

672

673

674

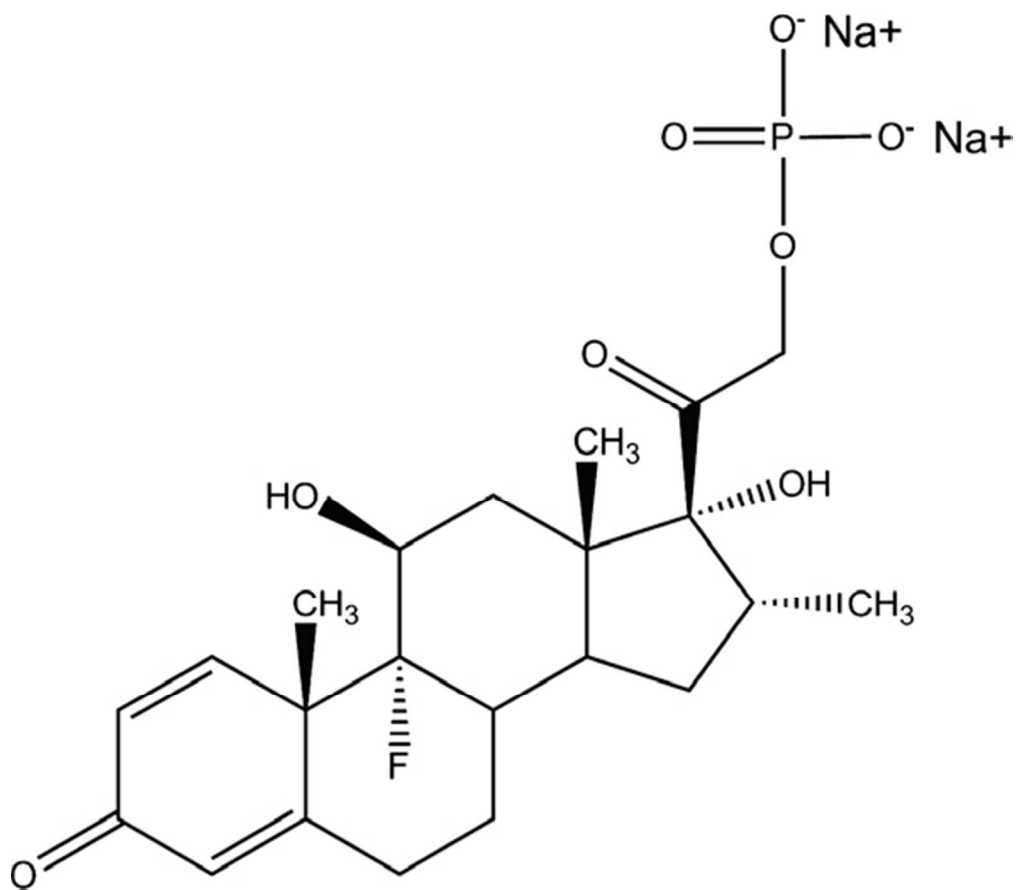


Figure 1  
156x136mm (96 x 96 DPI)

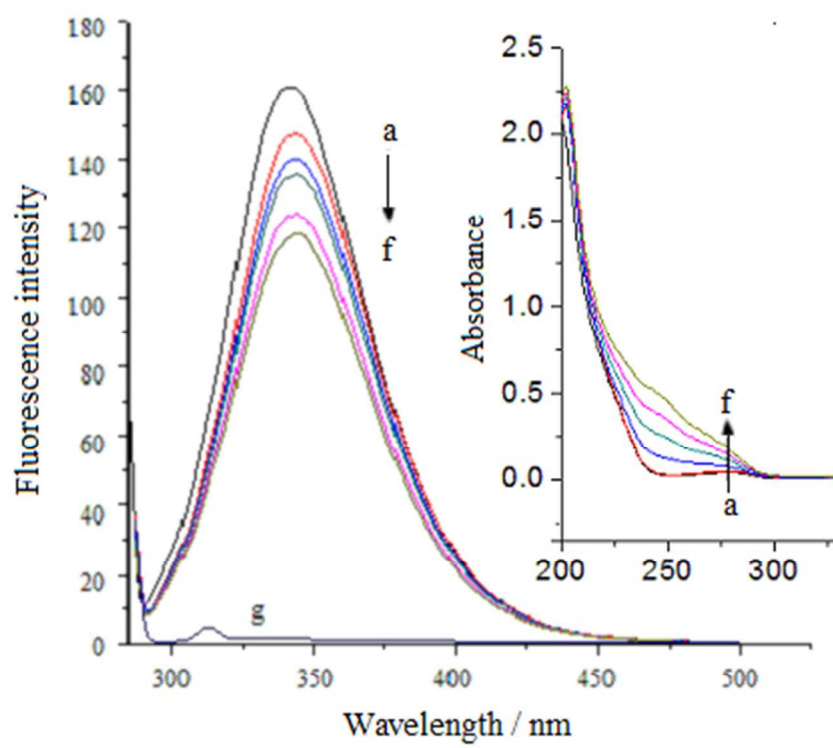


Figure 2  
115x105mm (96 x 96 DPI)

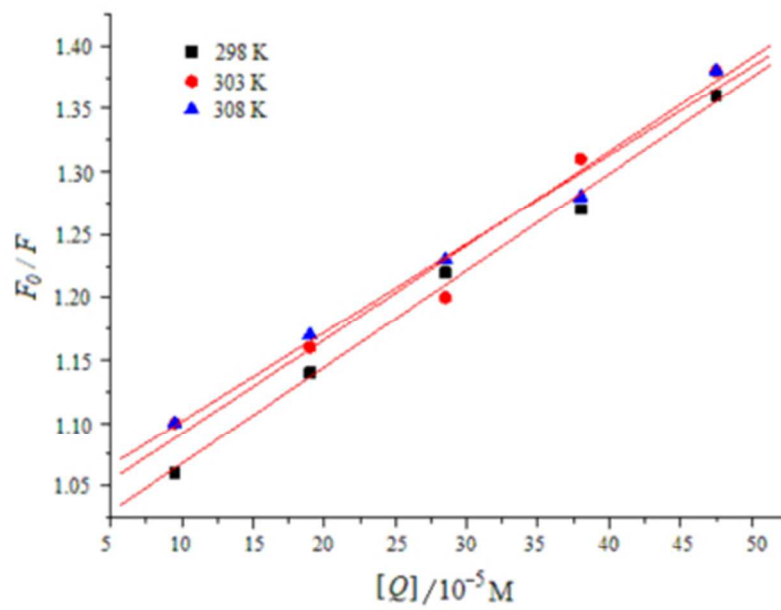


Figure 3  
109x89mm (96 x 96 DPI)

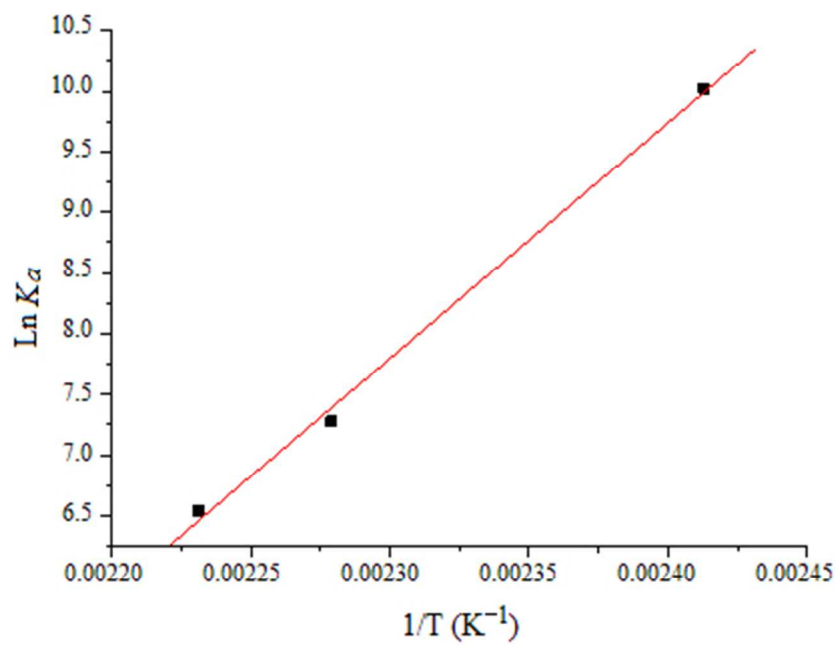


Figure 4  
123x94mm (96 x 96 DPI)

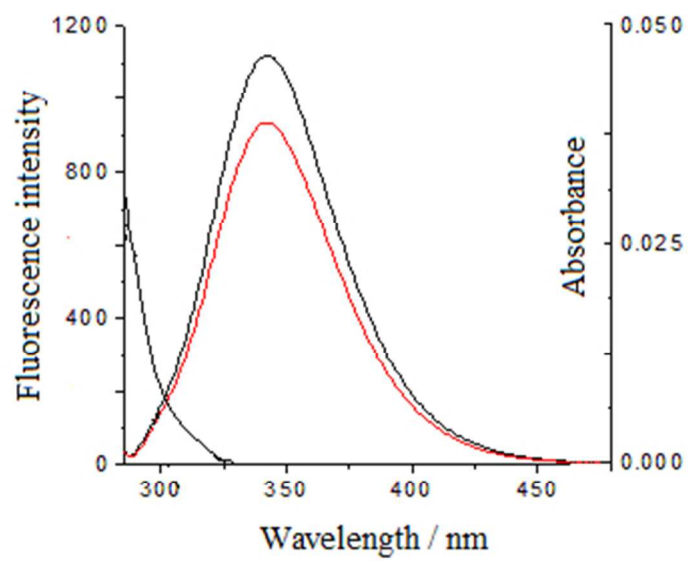


Figure 5  
95x85mm (96 x 96 DPI)

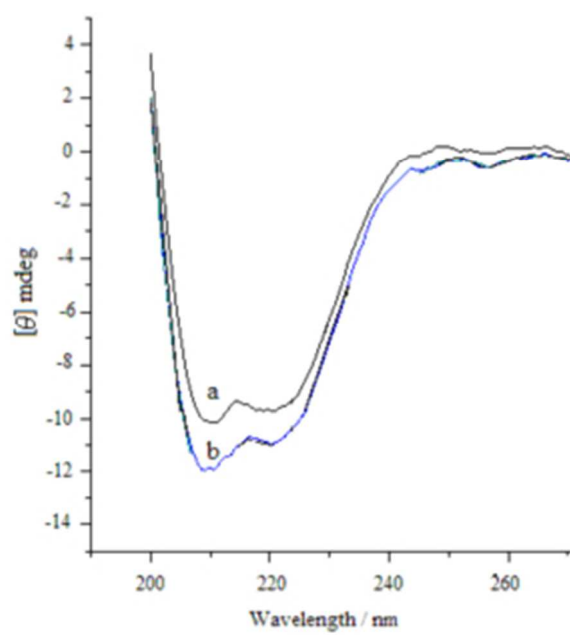


Figure 6  
83x86mm (96 x 96 DPI)

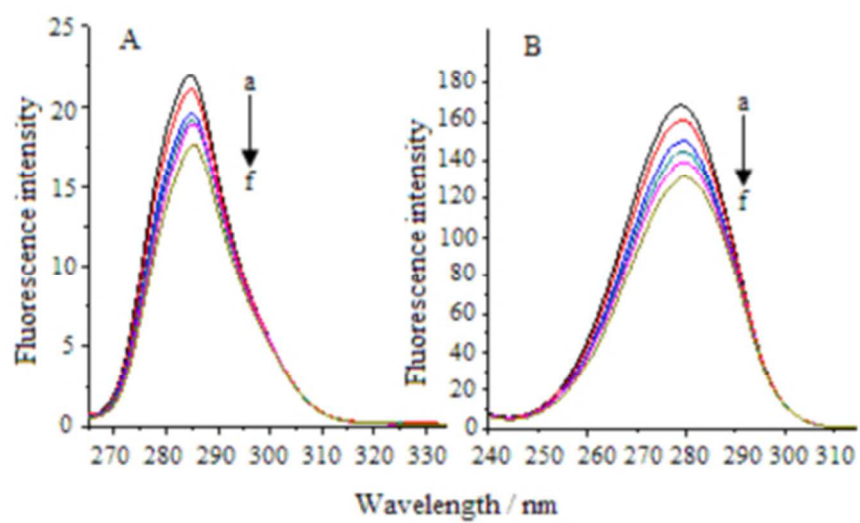


Figure 7  
119x79mm (96 x 96 DPI)

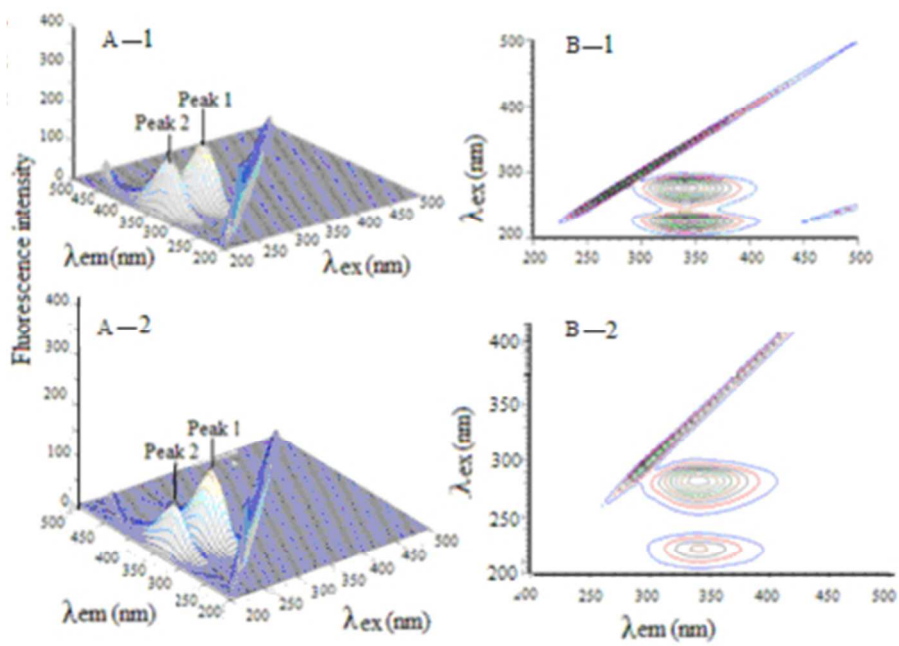


Figure 8  
120x87mm (96 x 96 DPI)

## Graphical abstract

